AIAA JOURNAL
Vol. 41, No. 8, August 2003

Sandwich-Plate Vibration Analysis: Three-Layer Quasi-Three-Dimensional Finite Element Model

Airton Nabarrete*
Centro Universitário Fundação Educacional Inaciana Pe Sabóia de Medeiros, 09850-901 São Bernardo do Campo, Brazil
Sergio Frascino M. de Almeida†
Instituto Tecnológico de Aeronáutica, 12228-900 São José dos Campos, Brazil
and
Jorn S. Hansen‡
University of Toronto, Toronto, Ontario M3H 5T6, Canada

A three-layer finite element model for the vibration analysis of sandwich plates with laminated composite face sheets is evaluated. In the model the face sheets are represented as Reissner–Mindlin plates, and the core is modeled as a three-dimensional continuum. This representation allows accurate modeling for a wide range of core types. The three-dimensional problem is reduced to two dimensions by analytical through-thickness integration of the energy expressions for the evaluation of mass and stiffness matrices. The results from this model are compared to finite element results based on solid elements, classical sandwich analysis, and classical plate theory. The objective in the work is to compare natural frequency and mode shape predictions using these models for a broad range of core stiffness. When large differences between face sheet and core stiffness are present, it is illustrated that traditional laminate theories yield significant inaccuracy. Moreover, unlike plate models, the present theory is also capable of representing a variety of three-dimensional boundary conditions. Furthermore, compared to solid models, the present laminated model avoids numerical problems as a result of three-dimensional element aspect ratio. Therefore, the present model provides a powerful general tool for the analysis of natural modes and frequencies of sandwich plates.

Nomenclature

A, B, D	=	in-plane, coupled bending-stretching and bending stiffness matrices
$\bar{A}, \bar{B}, \bar{D}, \bar{E}, \bar{F}, \bar{G}, \bar{H}$	=	stiffness matrices of the core
A^*	=	shear stiffness of the face sheets
$a_i, b_i, c_i, d_i, e_i, f_i, l_i, m_i, n_i$	=	bicubic trial functions of x and y
$\bar{C}_{ij}$	=	elastic moduli of the core
D	=	stiffness matrix
$\boldsymbol{e}$	=	strain vector
H	=	functional
I_i	=	mass and inertia moments
K, M	=	stiffness and mass matrices
k	=	layer number
N	=	finite element interpolation functions matrix
$\bar{Q}, \bar{Q}_M, \bar{Q}_S$	=	elastic matrices for face sheets
Q_{ij}	=	elastic moduli of the face sheets
T_i	=	transformation matrices
t_i	=	local coordinates along the thickness
U, T	=	strain and kinetic energy
$\boldsymbol{U}_i$	=	vector of displacement amplitudes
u, v, w	=	displacement functions of sandwich plate
$\bar{u}$	=	finite element displacements
u_i, v_i, w_i	=	through-thickness nodal displacements
V	=	volume of the plate
x, y, z	=	plate coordinates
$\bar{\varepsilon}$	=	arbitrary z coordinate in-plane strain vector
$\varepsilon_i, \gamma_{ij}$	=	strains
$\varepsilon_0, \boldsymbol{\kappa}_i, \boldsymbol{\Gamma}$	=	in-plane strain, curvature, and out-of-plane strain vectors
ρ	=	density
σ_i, τ_{ij}	=	stresses
ω_i	=	natural frequencies

Subscripts

b, c, t	=	bottom face sheet, core, and top face sheet

Introduction

SANDWICH plates are very popular for structural purposes because of the high stiffness-to-weight and strength-to-weight ratios. Often, accurate sandwich-plate analyses are difficult to achieve because of the large differences between face sheet and core stiffness that yield significance transverse shear effects in the core. A sandwich structure therefore requires a more sophisticated model than classical laminated-plate theory. Therefore, in an effort to improve solution accuracy, three-dimensional analyses are often used for sandwich structures. For example, a three-dimensional analysis is considered necessary when calculating the vibration modes and natural frequencies for sandwich plates because variations in vibration modes can result when core properties are altered. Also, transverse flexibility of the core can change the shape of traditional vibration modes or produce unanticipated modes with very low natural frequencies. On the other hand, three-dimensional finite element analysis is often not a viable alternative as thin face sheets and thick cores imply the use of many elements or else the introduction of numerical error through the use of unacceptable three-dimensional element aspect ratios.

Many authors have tried to describe sandwich-plate behavior based on improved solutions of laminated Reissner–Mindlin plate theory. Reissner[1] described a sandwich plate model with two face sheets having only membrane stiffness and a core having only

Received 9 May 2002; revision received 29 January 2003; accepted for publication 24 February 2003.

*Professor, Department of Mechanics; airtonn@fei.edu.br.
†Professor, Department of Mechanical Engineering; frascino@mec.ita.cta.br.
‡Professor, Institute for Aerospace Studies, 4925 Dufferin Street; hansen@utias.utoronto.ca.

transverse shear stiffness. Allen,[2] Plantema,[3] and Ojalvo[4] assumed the in-plane displacement of the core to be linear through the thickness. Holt and Webber[5] and Monforton and Ibrahim[6] demonstrated an analysis of a sandwich beam where the core had negligible in-plane stiffness. Frostig et al.[7] developed the analysis of the core deformations by a superposition approach where the effects of shear and thickness of the core were treated separately in an analytical method. Frostig and Baruch[8,9] enhanced their deformation model of the core based on variational principles and the introduction of high-order terms to describe the nonlinear patterns of the core through-thickness deformation. Nevertheless, the in-plane rigidity of the core was ignored because of complexity in the analytical formulation. Thomsen[10] presented the model of the core of a rectangular sandwich plate using a two-parameter elastic foundation approach to treat the problem of local bending deformation. Oskooei and Hansen[11] developed a three-layer quasi-three-dimensional finite element for static analysis of sandwich plates, where the face sheets were modeled using Reissner–Mindlin plate theory and the core modeled as a three-dimensional continuum. The presented formulation used a mixed form of the through-thickness fields for the core displacements. The u and v deflections are modeled as cubic functions and w deflection as a quadratic functions of z; all variables are bicubics with respect to x and y. For the face sheets the same cubic functions are adopted for deflections in x and y directions; thus, compatibility is guaranteed in the assembly of face sheets and core. This representation allows accurate modeling of static problems for a wide range of core and face-sheet stiffness.

The present work intends to extend the use of the three-layer quasi-three-dimensional finite element developed by Oskooei and Hansen[11] to solve the free-vibration problem of a sandwich plate. In the element formulation through-thickness integration of strain and kinetic energies is completed analytically; this gives the appearance of a two-dimensional finite element procedure and leads to computational efficiency. A FORTRAN code was generated, and a comparison of results was made between this formulation, three-dimensional finite elements, classical sandwich analysis, and classical plate theory. The presented results are the natural frequencies and mode shape predictions using a broad range of core stiffness. When large differences between face sheet and core stiffness are present, the current model always provides good agreement with refined three-dimensional finite element results, whereas traditional laminate theories yield significant inaccuracy. If compared with solid models of sandwich plates with thin face sheets and thick core, the present three-layer quasi-three-dimensional model avoids numerical problems associated with three-dimensional element aspect ratios.

Mathematical Formulation

The current formulation uses the model developed by Oskooei and Hansen.[11] The sandwich-plate reference surface is placed at the geometric middle surface of the core, as shown in Fig. 1. The face sheets include transverse shear effects that are consistent with a Reissner–Mindlin model (u_0, v_0, w_0, ψ_x, ψ_y). This allows capture of face-sheet delamination and face-sheet/core disbonding effects. The face-sheet displacements u_0, v_0, and w_0 are written with respect to

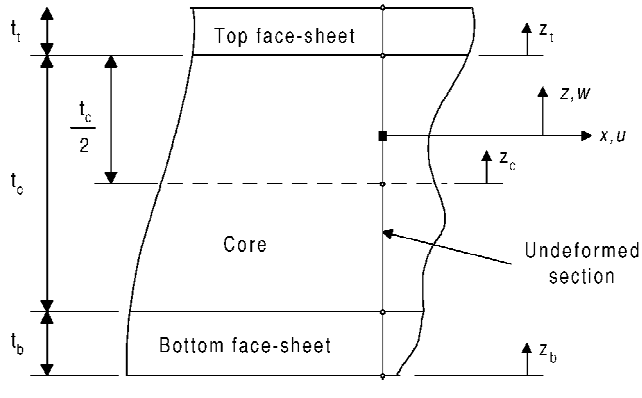

Fig. 1 Cross section of the sandwich plate.

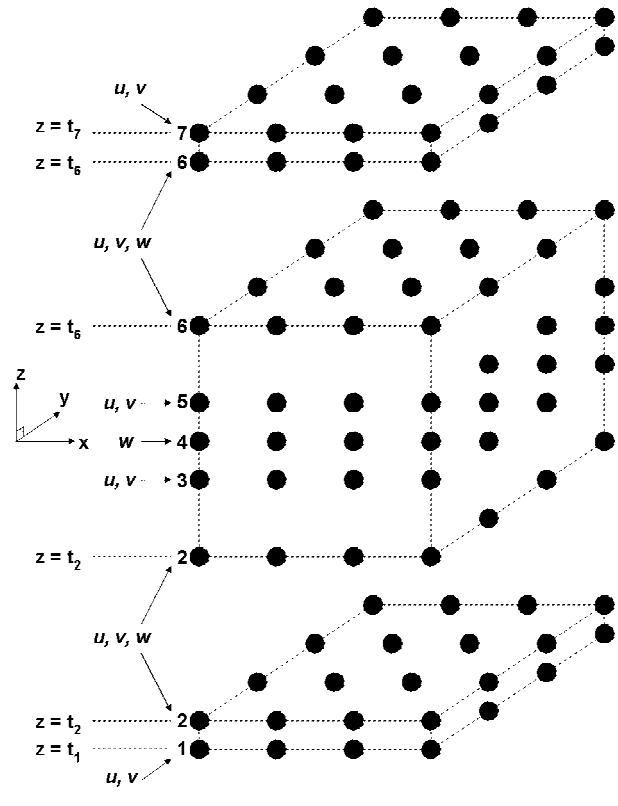

Fig. 2 Schematic of one element (through-thickness degrees of freedom).

the interface of that face sheet with the core, whereas the face-sheet rotation variables ψ_x and ψ_y are expressed as relative displacements u and v between bottom and top surface of a particular face sheet. This allows simpler through-thickness assembly using standard finite element ideas. Because the middle of the core is used as the formulation reference surface, there is inherent coupling between the membrane and bending effects of the face sheets, even for a linear analysis of symmetric laminates.

Based on the characteristics of a sandwich structure, Oskooei and Hansen[11] proposed that the core displacements u and v be modeled as cubic functions of z while w should be modeled as a quadratic in z. With these assumptions good accuracy is guaranteed for plates involving both light metallic honeycomb and flexible foam cores. This formulation does not set the core in-plane stiffness to zero as done by Frostig and Baruch[9] and Thomsen[10]; however, by adopting the trial functions as indicated, the strain energy corresponding to the in-plane stiffness has a negligible effect and will not induce artificial stiffening. The current trial functions also avoid shear locking difficulties; these functions are similar to finite element trial functions in which the order of in-plane approximations are chosen to avoid shear locking in a Reissner–Mindlin formulation.

Different through-thickness displacement models are adopted for the face sheets and the core. Thus, in order to develop the finite element representation it is convenient to separate the plate into three parts, the bottom face sheet, the core, and the top face sheet. The aim in this separation is to carry out an analytical through-thickness integration with respect to z using the core middle surface as the reference and thereby effectively reduce the model to two dimensions (x, y).

Figure 2 shows the through-thickness nodal arrangement of the top and bottom face sheets as well as the core. In addition, the degrees of freedom associated with each node are illustrated.

Kinematic Equations

Bicubic trial functions are used to model the in-plane (x, y) displacements characteristics. The use of bicubic trial functions leads to an extremely accurate formulation. For each layer the trial functions are represented by the following.

Bottom plate:

$$u(x,y,z) = a_0(x,y) + a_1(x,y)z$$
$$v(x,y,z) = b_0(x,y) + b_1(x,y)z, \qquad w(x,y,z) = l_0(x,y) \quad (1)$$

Core:

$$u(x,y,z) = c_0(x,y) + c_1(x,y)z + c_2(x,y)z^2 + c_3(x,y)z^3$$
$$v(x,y,z) = d_0(x,y) + d_1(x,y)z + d_2(x,y)z^2 + d_3(x,y)z^3$$
$$w(x,y,z) = m_0(x,y) + m_1(x,y)z + m_2(x,y)z^2 \quad (2)$$

Top plate:

$$u(x,y,z) = e_0(x,y) + e_1(x,y)z$$
$$v(x,y,z) = f_0(x,y) + f_1(x,y)z, \qquad w(x,y,z) = n_0(x,y) \quad (3)$$

Both top and bottom face sheets have a similar formulation. The following presents the formulation for the bottom face sheet. The strain components are

$$\varepsilon_x = a_{0,x} + z a_{1,x}, \qquad \varepsilon_y = b_{0,y} + z b_{1,y}$$
$$\gamma_{xy} = a_{0,y} + b_{0,x} + z(a_{1,y} + b_{1,x})$$
$$\gamma_{zx} = a_1 + l_{0,x}, \qquad \gamma_{yz} = b_1 + l_{0,y} \quad (4)$$

Expressions (4) are grouped as vectors involving in-plane strains, curvatures, and out-of-plane shear strains:

$$\{\bar{\varepsilon}\}_b = \begin{Bmatrix} \varepsilon_x \\ \varepsilon_y \\ \gamma_{xy} \end{Bmatrix} = \{\varepsilon_0\} + z\{\kappa\} = \begin{Bmatrix} a_{0,x} \\ b_{0,y} \\ a_{0,y} + b_{0,x} \end{Bmatrix} + z \begin{Bmatrix} a_{1,x} \\ b_{1,y} \\ a_{1,y} + b_{1,x} \end{Bmatrix} \quad (5)$$

$$\{\Gamma\}_b = \begin{Bmatrix} \gamma_{zx} \\ \gamma_{yz} \end{Bmatrix} = \begin{Bmatrix} a_1 + l_{0,x} \\ b_1 + l_{0,y} \end{Bmatrix} \quad (6)$$

The core strain components are written as

$$\varepsilon_x = c_{0,x} + z c_{1,x} + z^2 c_{2,x} + z^3 c_{3,x}$$
$$\varepsilon_y = d_{0,y} + z d_{1,y} + z^2 d_{2,y} + z^3 d_{3,y}, \qquad \varepsilon_z = m_1 + 2z m_2$$
$$\gamma_{xy} = c_{0,y} + z c_{1,y} + z^2 c_{2,y} + z^3 c_{3,y} + d_{0,x} + z d_{1,x} + z^2 d_{2,x} + z^3 d_{3,x}$$
$$\gamma_{zx} = c_1 + 2z c_2 + 3z^2 c_3 + m_{0,x} + z m_{1,x} + z^2 m_{2,x}$$
$$\gamma_{yz} = d_1 + 2z d_2 + 3z^2 d_3 + m_{0,y} + z m_{1,y} + z^2 m_{2,y} \quad (7)$$

which are arranged in a vector form as

$$\{\varepsilon\}_c = \begin{Bmatrix} \varepsilon_x \\ \varepsilon_y \\ \varepsilon_z \\ \gamma_{xy} \\ \gamma_{zx} \\ \gamma_{yz} \end{Bmatrix} = \begin{Bmatrix} c_{0,x} \\ d_{0,x} \\ m_1 \\ c_{0,y} + d_{0,x} \\ c_1 + m_{0,x} \\ d_1 + m_{0,y} \end{Bmatrix} + z \begin{Bmatrix} c_{1,x} \\ d_{1,y} \\ 2m_2 \\ c_{1,y} + d_{1,x} \\ 2c_2 + m_{1,x} \\ 2d_2 + m_{1,y} \end{Bmatrix}$$
$$+ z^2 \begin{Bmatrix} c_{2,x} \\ d_{2,y} \\ 0 \\ c_{2,y} + d_{2,x} \\ 3c_3 + m_{2,x} \\ 3d_3 + m_{2,y} \end{Bmatrix} + z^3 \begin{Bmatrix} c_{3,x} \\ d_{3,y} \\ 0 \\ c_{3,y} + d_{3,x} \\ 0 \\ 0 \end{Bmatrix} \quad (8)$$

$$\{\varepsilon\}_c = \{\varepsilon_0\} + z\{\kappa_1\} + z^2\{\kappa_2\} + z^3\{\kappa_3\} \quad (9)$$

Constitutive Equations

The face sheets can themselves be a composite laminate. The individual lamina is modeled having orthotropic material characteristics and is assumed to be in a state of plane stress; the transformed constitutive relation for any face-sheet lamina is

$$\begin{Bmatrix} \sigma_x \\ \sigma_y \\ \tau_{xy} \\ \tau_{zx} \\ \tau_{yz} \end{Bmatrix}_k = \left[\begin{array}{ccc|cc} \bar{Q}_{11} & \bar{Q}_{12} & \bar{Q}_{16} & 0 & 0 \\ \bar{Q}_{12} & \bar{Q}_{22} & \bar{Q}_{26} & 0 & 0 \\ \bar{Q}_{16} & \bar{Q}_{26} & \bar{Q}_{66} & 0 & 0 \\ \hline 0 & 0 & 0 & \bar{Q}_{55} & \bar{Q}_{45} \\ 0 & 0 & 0 & \bar{Q}_{45} & \bar{Q}_{44} \end{array}\right]_k \begin{Bmatrix} \varepsilon_x \\ \varepsilon_y \\ \gamma_{xy} \\ \gamma_{zx} \\ \gamma_{yz} \end{Bmatrix}_k \quad (10)$$

where the subscript k indicates the numbering of the face-sheet lamina. The preceding matrix was partitioned to separate the in-plane and out-of-plane components

$$\begin{Bmatrix} \sigma_x \\ \sigma_y \\ \tau_{xy} \\ \tau_{zx} \\ \tau_{yz} \end{Bmatrix}_k = \begin{bmatrix} [\bar{Q}_M] & [0] \\ [0] & [\bar{Q}_S] \end{bmatrix}_k \begin{Bmatrix} \{\bar{\varepsilon}\} \\ \{\Gamma\} \end{Bmatrix}_k \quad (11)$$

The core is modeled as an orthotropic material; the transformed constitutive relation is

$$\begin{Bmatrix} \sigma_x \\ \sigma_y \\ \sigma_z \\ \tau_{yz} \\ \tau_{zx} \\ \tau_{xy} \end{Bmatrix}_c = \begin{bmatrix} \bar{C}_{11} & \bar{C}_{12} & \bar{C}_{13} & 0 & 0 & \bar{C}_{16} \\ & \bar{C}_{22} & \bar{C}_{23} & 0 & 0 & \bar{C}_{26} \\ & & \bar{C}_{33} & 0 & 0 & \bar{C}_{36} \\ & & & \bar{C}_{44} & \bar{C}_{45} & 0 \\ & & & & \bar{C}_{55} & 0 \\ Sym & & & & & \bar{C}_{66} \end{bmatrix}_c \begin{Bmatrix} \varepsilon_x \\ \varepsilon_y \\ \varepsilon_z \\ \gamma_{yz} \\ \gamma_{zx} \\ \gamma_{xy} \end{Bmatrix}_c \quad (12)$$

Variational Formulation

The objective is to determine the natural frequencies and modes shapes of free-vibration problems; the appropriate motion equations are derived using Hamilton's principle:

$$\delta H = \int_t^{t+\Delta t} \delta(T - U)\,\mathrm{d}t = 0 \quad (13)$$

The total strain energy is the sum of the face sheets and core strain energies. Using the vector form developed earlier, the strain energy for the bottom face sheet becomes

$$U_b = \frac{1}{2}\int_A \left\{ \sum_{k=1}^{nb} \int_{z_{k-1}}^{z_k} \begin{Bmatrix} \{\bar{\varepsilon}\} \\ \{\Gamma\} \end{Bmatrix}_k^T \begin{bmatrix} [\bar{Q}_M] & [0] \\ [0] & [\bar{Q}_S] \end{bmatrix}_k \begin{Bmatrix} \{\bar{\varepsilon}\} \\ \{\Gamma\} \end{Bmatrix}_k \mathrm{d}z \right\}_b \mathrm{d}A \quad (14)$$

which is integrated analytically through the thickness yielding

$$U_b = \frac{1}{2}\int_A \begin{Bmatrix} \{\varepsilon_0\} \\ \{\kappa\} \\ \{\Gamma\} \end{Bmatrix}_b^T \begin{bmatrix} [A] & [B] & [0] \\ [B] & [D] & [0] \\ [0] & [0] & [A^*] \end{bmatrix}_b \begin{Bmatrix} \{\varepsilon_0\} \\ \{\kappa\} \\ \{\Gamma\} \end{Bmatrix}_b \mathrm{d}A \quad (15)$$

where

$$([A]_b, [B]_b, [D]_b) = \sum_{k=1}^{n_b} \int_{z_{k-1}}^{z_k} [\bar{Q}_M]_k (1, z, z^2)\,\mathrm{d}z \quad (16)$$

$$[A^*]_b = \sum_{k=1}^{n_b} \int_{z_{k-1}}^{z_k} [\bar{Q}_S]_k\,\mathrm{d}z \quad (17)$$

In the preceding equations, n_b is the number of plies in the bottom face sheet, whereas z_{k-1} and z_k are the lower and upper z coordinate of each ply.[12] The matrices $[A]$, $[B]$, $[D]$, and $[A^*]$ have the appearance of the standard results for laminated composite plates; however, it is important to note that there is an offset because the z reference surface is the core middle surface. The matrices $[A]$ and $[A^*]$ are not influenced by this offset. The matrix $[B]$ is a coupling matrix that is nonzero even when the face-sheet laminate is symmetric unlike in the usual laminated-plate scenario. In the current

representation through-thickness symmetry does not simplify the plate equations unless the entire sandwich structure is symmetric with respect to the core middle surface and until the face-sheet and core stiffness matrices are assembled.

The strain energy for the top face sheet has a formulation similar to expression (15). For the core the strain energy becomes

$$U_c = \frac{1}{2}\int_V \{\varepsilon\}_c^T [\bar{Q}]_c \{\varepsilon\}_c \, dV \tag{18}$$

Through-thickness integration yields

$$U_c = \frac{1}{2}\int_A \begin{Bmatrix} \{\varepsilon_0\} \\ \{\kappa_1\} \\ \{\kappa_2\} \\ \{\kappa_3\} \end{Bmatrix}_c^T \begin{bmatrix} [\bar{A}] & [\bar{B}] & [\bar{D}] & [\bar{E}] \\ [\bar{B}] & [\bar{D}] & [\bar{E}] & [\bar{F}] \\ [\bar{D}] & [\bar{E}] & [\bar{F}] & [\bar{G}] \\ [\bar{E}] & [\bar{F}] & [\bar{G}] & [\bar{H}] \end{bmatrix}_c \begin{Bmatrix} \{\varepsilon_0\} \\ \{\kappa_1\} \\ \{\kappa_2\} \\ \{\kappa_3\} \end{Bmatrix}_c dA \tag{19}$$

where

$$([\bar{A}], [\bar{B}], [\bar{D}], [\bar{E}], [\bar{F}], [\bar{G}], [\bar{H}])_c = \int_{-z_c}^{z_c} [\bar{Q}]_c (1, z, z^2, z^3, z^4, z^5, z^6)\, dz \tag{20}$$

In the preceding, $[\bar{A}]$, $[\bar{B}]$, $[\bar{D}]$, $[\bar{E}]$, $[\bar{F}]$, $[\bar{G}]$, and $[\bar{H}]$ are 6×6 matrices.

Note that $[\bar{A}]$, $[\bar{D}]$, $[\bar{F}]$, and $[\bar{H}]$ do not vanish even for a symmetric core. The total kinetic energy is given by

$$T = \frac{1}{2}\int_v \begin{Bmatrix} \dot{u} \\ \dot{v} \\ \dot{w} \end{Bmatrix}^T \begin{Bmatrix} \dot{u} \\ \dot{v} \\ \dot{w} \end{Bmatrix} \rho \, dV \tag{21}$$

The total kinetic energy is the sum of the face sheets and core kinetic energies. Evaluating the through-thickness integration for the bottom face sheet yields

$$T_b = \frac{1}{2}\int_A \begin{Bmatrix} \dot{a}_0 \\ \dot{b}_0 \\ \dot{l}_0 \\ \dot{a}_1 \\ \dot{b}_1 \end{Bmatrix}^T \begin{bmatrix} I_{1b} & 0 & 0 & I_{2b} & 0 \\ & I_{1b} & 0 & 0 & I_{2b} \\ & & I_{1b} & 0 & 0 \\ & & & I_{3b} & 0 \\ sym & & & & I_{3b} \end{bmatrix} \begin{Bmatrix} \dot{a}_0 \\ \dot{b}_0 \\ \dot{l}_0 \\ \dot{a}_1 \\ \dot{b}_1 \end{Bmatrix} dA \tag{22}$$

where

$$I_{1b}, I_{2b}, I_{3b} = \int_{t_1}^{t_2} (1, z, z^2)\rho_b \, dz \tag{23}$$

The top face sheet yields a similar result to expressions (22) and (23). The kinetic energy for the core after through-thickness integration yields

$$T_c = \frac{1}{2}\int_A \begin{Bmatrix} \dot{c}_0 \\ \dot{d}_0 \\ \dot{m}_0 \\ \dot{c}_1 \\ \dot{d}_1 \\ \dot{m}_1 \\ \dot{c}_2 \\ \dot{d}_2 \\ \dot{m}_2 \\ \dot{c}_3 \\ \dot{d}_3 \end{Bmatrix}^T \begin{bmatrix} I_{1c} & 0 & 0 & 0 & 0 & 0 & I_{2c} & 0 & 0 & 0 & 0 \\ & I_{1c} & 0 & 0 & 0 & 0 & 0 & I_{2c} & 0 & 0 & 0 \\ & & I_{1c} & 0 & 0 & 0 & 0 & 0 & I_{2c} & 0 & 0 \\ & & & I_{2c} & 0 & 0 & 0 & 0 & 0 & I_{3c} & 0 \\ & & & & I_{2c} & 0 & 0 & 0 & 0 & 0 & I_{3c} \\ & & & & & I_{2c} & 0 & 0 & 0 & 0 & 0 \\ & & & & & & I_{3c} & 0 & 0 & 0 & 0 \\ & & & & & & & I_{3c} & 0 & 0 & 0 \\ & & & & & & & & I_{3c} & 0 & 0 \\ & & & & & & & & & I_{4c} & 0 \\ sym & & & & & & & & & & I_{4c} \end{bmatrix} \begin{Bmatrix} \dot{c}_0 \\ \dot{d}_0 \\ \dot{m}_0 \\ \dot{c}_1 \\ \dot{d}_1 \\ \dot{m}_1 \\ \dot{c}_2 \\ \dot{d}_2 \\ \dot{m}_2 \\ \dot{c}_3 \\ \dot{d}_3 \end{Bmatrix} dA \tag{24}$$

Some core inertia contributions vanish because the z reference is the middle of the core.

The core inertia terms are written as

$$I_{1c}, I_{2c}, I_{3c}, I_{4c} = \int_{-t_0}^{t_0} (1, z^2, z^4, z^6)\rho_c \, dz \tag{25}$$

Finite Element Formulation

A finite element formulation is developed to solve the free-vibration problem. A two-dimensional isoparametric bicubic element with 16 nodes using standard Lagrange interpolation functions was implemented in a FORTRAN code. A shear correction factor of $\frac{5}{6}$ is adopted for both face sheets. With this finite element formulation the top and bottom face sheets do not suffer from shear locking, and no special techniques such as reduced integration need be applied for the integration of the stiffness matrix[13]; therefore, a standard 16-point Gauss quadrature scheme is used. Also, the current formulation is applicable for both thick and thin composite face sheets. As demonstrated by Oskooei and Hansen,[11] the transformation of polynomial coefficients in terms of through-thickness nodal displacements helps the assembly of the face sheets and core stiffness matrix.

For the bottom face sheet the transformation to through-thickness nodal displacements becomes

$$\begin{Bmatrix} a_0 \\ b_0 \\ l_0 \\ a_1 \\ b_1 \end{Bmatrix} = \frac{1}{t_2 - t_1} \begin{bmatrix} t_2 & 0 & -t_1 & 0 & 0 \\ 0 & t_2 & 0 & -t_1 & 0 \\ 0 & 0 & 0 & 0 & t_2 - t_1 \\ -1 & 0 & 1 & 0 & 0 \\ 0 & -1 & 0 & 1 & 0 \end{bmatrix} \begin{Bmatrix} u_1 \\ v_1 \\ u_2 \\ v_2 \\ w_2 \end{Bmatrix}$$

$$= [T_1]_b \begin{Bmatrix} u_1 \\ v_1 \\ u_2 \\ v_2 \\ w_2 \end{Bmatrix} \tag{26}$$

For the top face sheet the transformation to through-thickness nodal displacements becomes

$$\begin{Bmatrix} e_0 \\ f_0 \\ n_0 \\ e_1 \\ f_1 \end{Bmatrix} = \frac{1}{t_7 - t_6} \begin{bmatrix} t_7 & 0 & 0 & -t_6 & 0 \\ 0 & t_7 & 0 & 0 & -t_6 \\ 0 & 0 & t_7 - t_6 & 0 & 0 \\ -1 & 0 & 0 & 1 & 0 \\ 0 & -1 & 0 & 0 & 1 \end{bmatrix} \begin{Bmatrix} u_6 \\ v_6 \\ w_6 \\ u_7 \\ v_7 \end{Bmatrix}$$

$$= [T_1]_t \begin{Bmatrix} u_6 \\ v_6 \\ w_6 \\ u_7 \\ v_7 \end{Bmatrix} \tag{27}$$

For the core the transformation matrices for the through-thickness nodal displacements u and v are

$$\begin{Bmatrix} c_0 \\ c_1 \\ c_2 \\ c_3 \end{Bmatrix} = \frac{1}{16 \cdot t_6^3} \begin{bmatrix} -t_6^3 & 9 \cdot t_6^3 & 9 \cdot t_6^3 & -t_6^3 \\ t_6^2 & -27 \cdot t_6^2 & 27 \cdot t_6^2 & -t_6^2 \\ 9 \cdot t_6 & -9 \cdot t_6 & -9 \cdot t_6 & 9 \cdot t_6 \\ -9 & 27 & -27 & 9 \end{bmatrix} \begin{Bmatrix} u_2 \\ u_3 \\ u_5 \\ u_6 \end{Bmatrix}$$

$$= [T_1]_c \begin{Bmatrix} u_2 \\ u_3 \\ u_5 \\ u_6 \end{Bmatrix} \tag{28}$$

$$\begin{Bmatrix} d_0 \\ d_1 \\ d_2 \\ d_3 \end{Bmatrix} = [T_1]_c \begin{Bmatrix} v_2 \\ v_3 \\ v_5 \\ v_6 \end{Bmatrix} \tag{29}$$

The transformation matrix for w is

$$\begin{Bmatrix} m_0 \\ m_1 \\ m_2 \end{Bmatrix} = \frac{1}{16 \cdot t_6^2} \begin{bmatrix} 0 & 16 \cdot t_6^2 & 0 \\ -8 \cdot t_6 & 0 & 8 \cdot t_6 \\ 8 & -16 & 8 \end{bmatrix} \begin{Bmatrix} w_2 \\ w_4 \\ w_6 \end{Bmatrix} = [T_2]_c \begin{Bmatrix} w_2 \\ w_4 \\ w_6 \end{Bmatrix} \tag{30}$$

In the same way the through-thickness nodal velocities are used in the assembly of the face-sheet and core mass matrices. The transformation of polynomial coefficient derivatives in terms of through-thickness nodal velocities are also obtained from the $[T_1]_b$, $[T_1]_t$, $[T_1]_c$, and $[T_2]_c$ transformation matrices for the bottom, top face sheet, and core, respectively. The sandwich stiffness and mass matrices have a total of 15 through-thickness displacements and velocity nodal variables, respectively. The coefficients (u_1, u_2, u_3, u_5, u_6, u_7, v_1, v_2, v_3, v_5, v_6, v_7, w_2, w_4, and w_6) represent 15 degrees of freedom for each node. Therefore there are 240 degrees of freedom corresponding to the 16 node elements.

The displacements at an arbitrary point within the domain of the pth element are written as

$$\{\bar{u}\}^T = [u_1 \;\; v_1 \;\; u_2 \;\; v_2 \;\; w_2 \;\; u_3 \;\; v_3 \;\; w_4 \;\; u_5 \;\; v_5 \;\; u_6 \;\; v_6 \;\; w_6 \;\; u_7 \;\; v_7] \tag{31}$$

These displacements in terms of element nodal displacements are expressed as

$$\{\bar{u}\} = \sum_{i=1}^{16} ([N]_i \{\bar{u}_i\}) = [N]\{\bar{u}\}_p \tag{32}$$

where $[N]$ is a 15×240 matrix of basis functions.

The vector $\{\bar{u}\}_p$ contains 240 element nodal degrees of freedom. The matrix of interpolation functions can also be used to relate the velocities at an arbitrary point with the element nodal velocities. The strain energy is written for n elements as[14]

$$U = \frac{1}{2} \sum_{p=1}^{n} \{\bar{u}\}_p^T [K_b]_p \{\bar{u}\}_p + \frac{1}{2} \sum_{p=1}^{n} \{\bar{u}\}_p^T [K_c]_p \{\bar{u}\}_p + \frac{1}{2} \sum_{p=1}^{n} \{\bar{u}\}_p^T [K_t]_p \{\bar{u}\}_p \tag{33}$$

In a similar manner the kinetic energy for n elements becomes

$$T = \frac{1}{2} \sum_{p=1}^{n} \{\dot{\bar{u}}\}_p^T [M_b]_p \{\dot{\bar{u}}\}_p + \frac{1}{2} \sum_{p=1}^{n} \{\dot{\bar{u}}\}_p^T [M_c]_p \{\dot{\bar{u}}\}_p + \frac{1}{2} \sum_{p=1}^{n} \{\dot{\bar{u}}\}_p^T [M_t]_p \{\dot{\bar{u}}\}_p \tag{34}$$

Eigenvalue Problem

Applying Hamilton's principle for n discrete finite elements, the motion equation becomes

$$[M]\{\ddot{\bar{u}}\} - [K]\{\bar{u}\} = \{0\} \tag{35}$$

Also, for simple harmonic motion

$$\{\bar{u}\} = \{\boldsymbol{U}_i\} e^{j\omega t}, \qquad \{\ddot{\bar{u}}\} = -\omega_i^2 \{\boldsymbol{U}_i\} e^{j\omega t} \tag{36}$$

Therefore, the eigenvalue problem defining the free-vibration problem becomes

$$\{[K] - \omega_i^2 \cdot [M]\} \cdot \{\boldsymbol{U}_i\} = \{0\} \tag{37}$$

where $[M]$ and $[K]$ are the global mass and stiffness matrices and $\{\boldsymbol{U}_i\}$ represents the corresponding mode of free vibration for the sandwich plate. The natural frequencies and mode shapes are determined using the subspace iteration method.[15]

Numerical Results

A FORTRAN code was developed to solve the free-vibration problem. This code allows any combination of plate geometry (sandwich-plate area, thickness of the face sheets, or the core, number of laminae for the face sheets), material properties (very soft core material, orthotropic or isotropic face sheets, etc.), and boundary conditions of the sandwich plate. This code was extensively tested to verify correctness and accuracy, and all tests showed excellent results.

A sandwich plate with aluminum face sheets and an isotropic homogeneous core are analyzed to demonstrate the capabilities of this formulation. The dimensions of the sandwich plate are given in Fig. 3 and the material properties in Table 1. Three different representations of clamped boundary conditions are considered for this plate. This allows the results of the current formulation to be compared to those of a sandwich beam because of the aspect ratio a/b. Figure 3a illustrates the first condition in which both face sheets at one edge are clamped, whereas the other edges are free. Figure 3b presents a sandwich plate with both face sheets clamped for two opposite edges, whereas the other two are free. Finally, Fig. 3c depicts a set of unsymmetrical boundary conditions for the sandwich plate, where the bottom face sheet is clamped at two opposite edges and the top face sheet is completely free.

The results from these analyses are compared with three other approaches when the boundary conditions permit. Comparisons are completed for a range of core stiffnesses and different boundary conditions. In all results core density is kept fixed as the core stiffness changes; this approach is adopted to isolate the influence of core stiffness. Results are presented for the least frequency vibration modes corresponding to flexure, torsion, and in-plane motion; these are not necessarily the least three natural frequencies.

The natural frequencies obtained for each vibration mode of the plates analyzed are summarized in Tables 2–10. In these tables the current quasi-three-dimensional model is compared with three other sets of results. In the tables the vibration mode is identified in the

Table 1 Dimensions and material properties of the sandwich-plate layers

Property	Face sheets	Core
Thickness, mm	1.0	8.0
Density, kg/m^3	2713	500
Young's modulus, MPa	68258	Variable
Poisson ratio	0.33	0.3

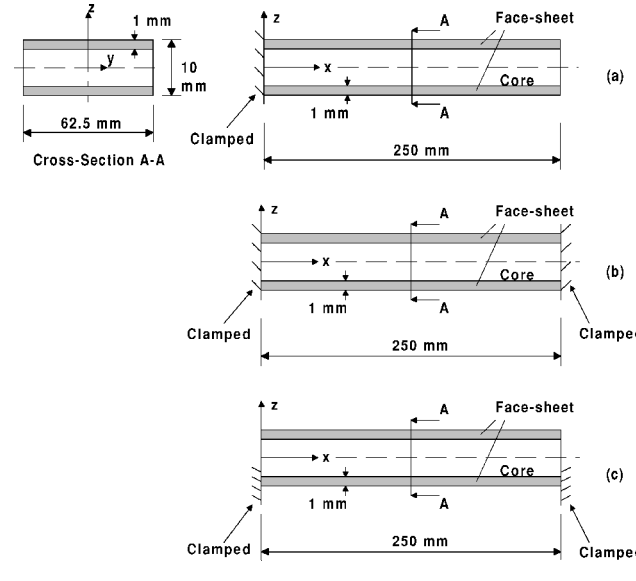

Fig. 3 Boundary conditions for the sandwich plate: a) both face sheets clamped at one edge; b) both face sheets clamped for two opposite edges; and c) bottom face sheet clamped for two opposite edges.

Table 2 First bending mode of one edge clamped at both face sheets

E_C, MPa	Frequency, Hz: Quasi-three-dimensional	Three-dimensional solid	Classical sandwich theory	Classical plate theory
10,000	166.5	166.8	166.0	166.9
3,000	157.2	157.5	156.3	158.8
1,000	152.1	152.4	149.9	156.4
301	143.1	143.4	137.3	155.6
151	133.5	133.7	124.2	155.4
66	115.7	115.9	102.3	155.3
30	94.0	94.2	78.7	155.2
10	63.9	64.1	49.8	155.2

Table 3 First torsion mode of one edge clamped at both face sheets

E_C, MPa	Frequency, Hz: Quasi-three-dimensional	Three-dimensional solid	Classical sandwich theory	Classical plate theory
10,000	1,160.0	1,155.8	1,133.5	1,214.6
3,000	991.6	988.1	936.7	1,142.4
1,000	810.4	807.3	733.6	1,119.9
301	587.3	586.3	513.1	1,111.8
151	472.7	472.6	408.7	1,110.1
66	362.2	362.6	310.5	1,109.1
30	284.5	285.1	241.7	1,108.6
10	213.9	214.7	179.1	1,108.4

Table 4 First in-plane mode of one edge clamped at both face sheets

E_C, MPa	Frequency, Hz: Quasi-three-dimensional	Three-dimensional solid	Classical sandwich theory	Classical plate theory
10,000	742.4	743.0	741.5	741.5
3,000	638.7	639.6	638.4	638.4
1,000	605.8	606.8	605.7	605.7
301	593.8	594.9	593.9	593.9
151	591.0	592.3	591.3	591.3
66	589.3	590.7	589.8	589.8
30	588.0	589.8	589.2	589.2
10	585.4	588.6	588.8	588.8

Table 5 First bending mode of both face sheet clamped at two opposite edges

E_C, MPa	Frequency, Hz: Quasi-three-dimensional	Three-dimensional solid	Classical sandwich theory	Classical plate theory
10,000	1,034.5	1,038.2	1,018.5	1,052.4
3,000	928.3	930.3	887.5	997.6
1,000	798.1	797.7	723.9	981.0
301	589.8	588.4	497.0	975.0
151	463.0	462.2	375.9	973.7
66	332.3	332.3	259.0	973.0
30	238.2	238.5	177.5	972.7
10	152.0	152.3	103.1	972.5

table caption; the core elastic modulus appears in the first column; the second column lists the natural frequencies obtained for this quasi-three-dimensional model; the third column presents the comparative frequencies from a three-dimensional Nastran calculation using solid elements; the fourth and fifth columns are obtained using classical sandwich analysis and classical plate theory, respectively. A FORTRAN code[16] for the free-vibration problem of composite laminates was used for these two last sets of results.

Table 6 First torsion mode of both face sheet clamped at two opposite edges

E_C, MPa	Frequency, Hz: Quasi-three-dimensional	Three-dimensional solid	Classical sandwich theory	Classical plate theory
10,000	2,454.8	2,448.2	2,378.8	2,597.9
3,000	2,042.6	2,032.8	1,901.3	2,436.5
1,000	1,623.2	1,614.0	1,455.5	2,385.7
301	1,180.8	1,179.2	1,043.7	2,367.3
151	980.5	982.4	868.2	2,363.3
66	796.8	801.4	701.2	2,361.0
30	657.5	664.4	560.9	2,360.1
10	483.8	493.7	379.6	2,359.5

Table 7 First in-plane mode of both face sheet clamped at two opposite edges

E_C, MPa	Frequency, Hz: Quasi-three-dimensional	Three-dimensional solid	Classical sandwich theory	Classical plate theory
10,000	3,612.8	3,618.2	3,658.8	3,658.8
7,000	3,415.7	3,421.8	3,449.0	3,449.0
5,000	3,277.2	3,283.7	3,301.7	3,301.7
3,000	3,131.9	3,138.9	3,147.6	3,147.6
1,000	2,976.5	2,985.5	2,985.4	2,985.4
301	2,910.6	2,926.7	2,926.7	2,926.6
151	2,882.4	2,909.6	2,913.9	2,913.9

Table 8 First bending mode of bottom face sheet clamped at two opposite edges

E_C, MPa	Frequency, Hz: Quasi-three-dimensional	Three-dimensional solid
10,000	704.9	657.0
3,000	623.9	588.4
1,000	558.5	538.0
301	464.8	455.2
151	393.9	388.2
66	302.8	300.2
30	228.8	223.8
10	144.9	144.8

Table 9 First torsion mode of bottom face sheet clamped at two opposite edges

E_C, MPa	Frequency, Hz: Quasi-three-dimensional	Three-dimensional solid
10,000	2,193.3	2,140.0
3,000	1,853.8	1,798.2
1,000	1,471.2	1,420.7
301	1,002.1	970.8
151	773.1	753.0
66	562.7	552.5
30	420.9	416.5
10	292.2	291.7

Table 10 First in-plane mode of bottom face sheet clamped at two opposite edges

E_C, MPa	Frequency, Hz: Quasi-three-dimensional	Three-dimensional solid
10,000	3,230.5	3,224.4
7,000	3,046.3	3,043.6
5,000	2,907.8	2,907.2
3,000	2,746.3	2,747.3
1,000	2,528.1	2,529.8
301	2,366.6	2,369.3
151	2,368.4	2,391.0

Influence of Core Stiffness

A key parameter studied using the current code is the variation of the core transverse stiffness. When the core transverse stiffness is high, as in a metallic honeycomb material, the sandwich structure can be analyzed using classical sandwich theories, and accurate results will be obtained. However, when the core transverse stiffness is low in comparison with the face sheets the same conclusion is not valid. With low core stiffness the face-sheet displacement field is affected, which results in a nonlinear displacement field in the core; the entire sandwich-plate thickness changes, and the core cross-sectional plane is distorted. Therefore, vibration modes consisting of a relative transverse displacement between the two face sheets can occur.

The results of Tables 2–7 are presented graphically in Figs. 4–9. The exact shape of the vibration modes depend on the core stiffness. However, for visualization purposes Figs. 4–9 show typical shapes of the corresponding vibration modes. It can be seen that there is excellent agreement between the present quasi-three-dimensional model results in comparison to the three-dimensional Nastran results. The models relating to classical sandwich analysis and classical plate theory have however much greater discrepancies for flexible cores. For bending modes in the y direction or the torsion modes, discrepancies are high when core transverse stiffness has values under 5% of the face-sheet values.

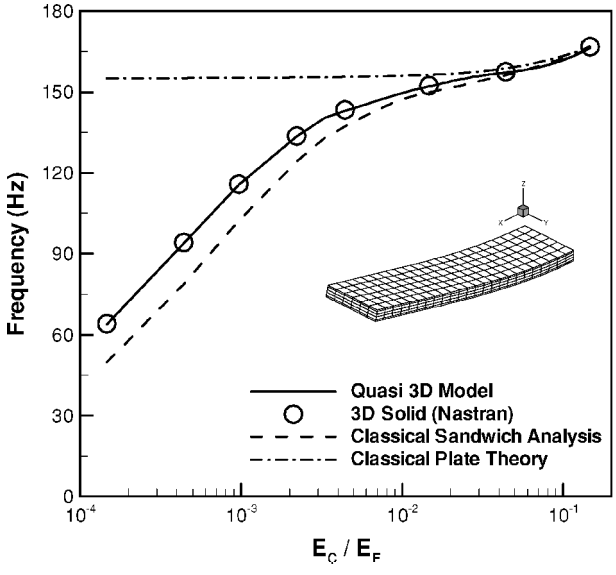

Fig. 4 First bending mode for both face sheets clamped at one edge.

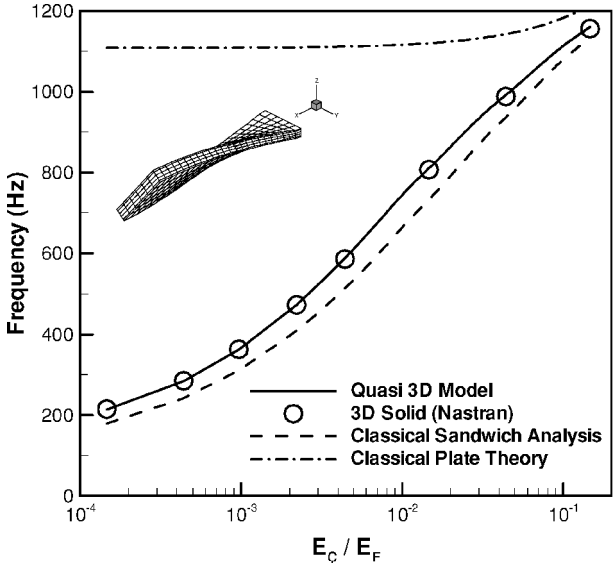

Fig. 5 First torsion mode for both face sheets clamped at one edge.

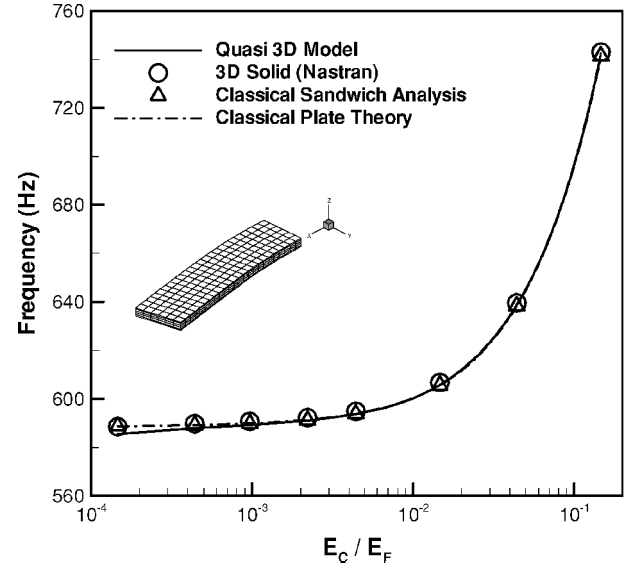

Fig. 6 First in-plane mode for both face sheets clamped at one edge.

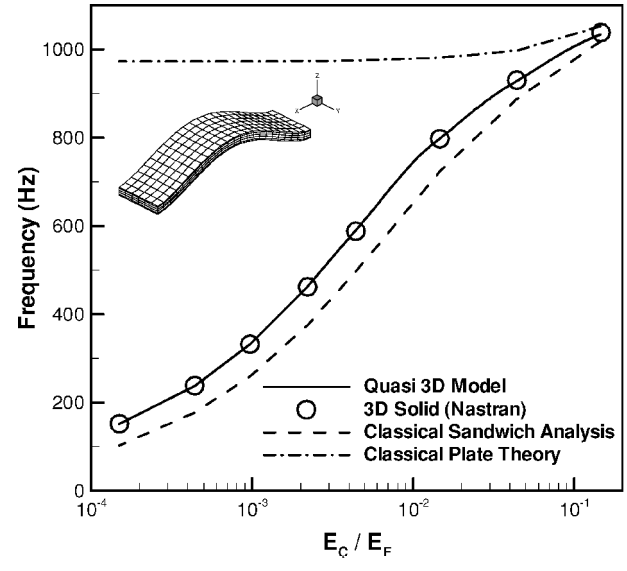

Fig. 7 First bending mode for both face sheets clamped at two opposite edges.

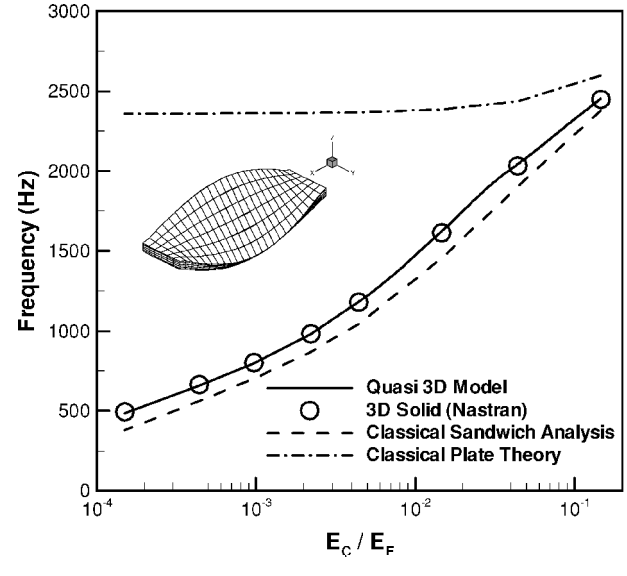

Fig. 8 First torsion mode for both face sheets clamped at two opposite edges.

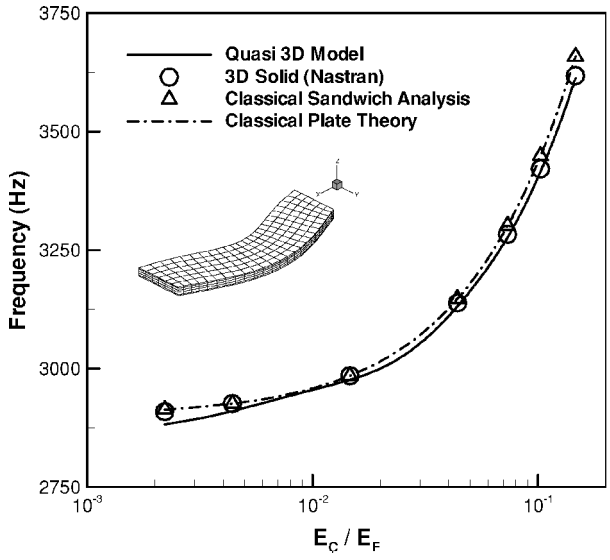

Fig. 9 First in-plane mode for both face sheets clamped at two opposite edges.

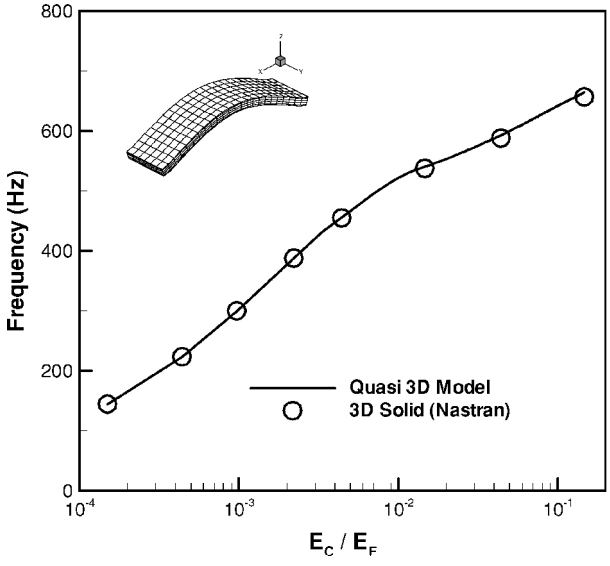

Fig. 10 First bending mode of bottom face sheet clamped at two opposite edges.

The present formulation yields excellent results compared to the three-dimensional Nastran results for a full range of core stiffness properties ranging from rigid to flexible; such a range includes metallic and nonmetallic honeycomb as well as plastic PVC foam materials. The currently developed formulation has a great accuracy advantage compared to classical plate theories when large variations of stiffness between the core and face sheets are present. Furthermore, for thin face sheets the current approach has an enormous computational advantage compared to three-dimensional calculations. Thus the current approach appears to represent a powerful computational tool for sandwich structures in which the core is very flexible compared to the face sheets.

Influence of Boundary Conditions

The accurate representation of boundary conditions can represent a difficulty problem for classical sandwich analysis or classical plate theory. In particular, boundary conditions that are not imposed symmetrically on both face sheets cannot be modeled. The quasi-three-dimensional formulation does not suffer from this difficulty. Tables 8–10 present results that show the influence of different boundary conditions for the face sheets and core. Classical sandwich analysis and classical plate theory cannot represent such a situation, and therefore no results were obtained. These results are also represented graphically in Figs. 10–12, where the comparison is made

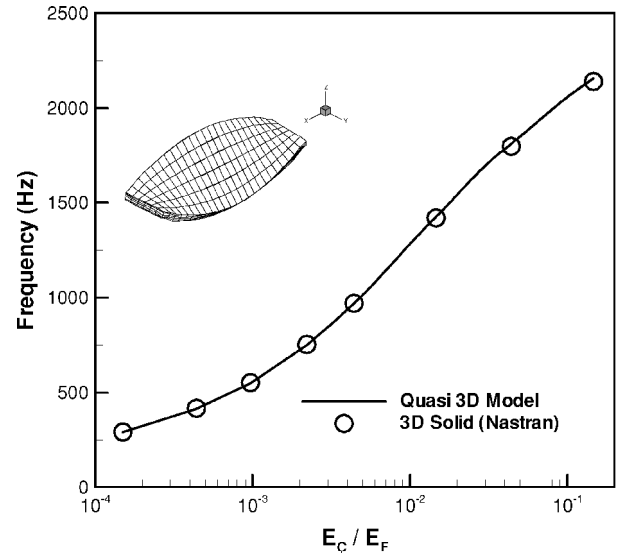

Fig. 11 First torsion mode of bottom face sheet clamped at two opposite borders.

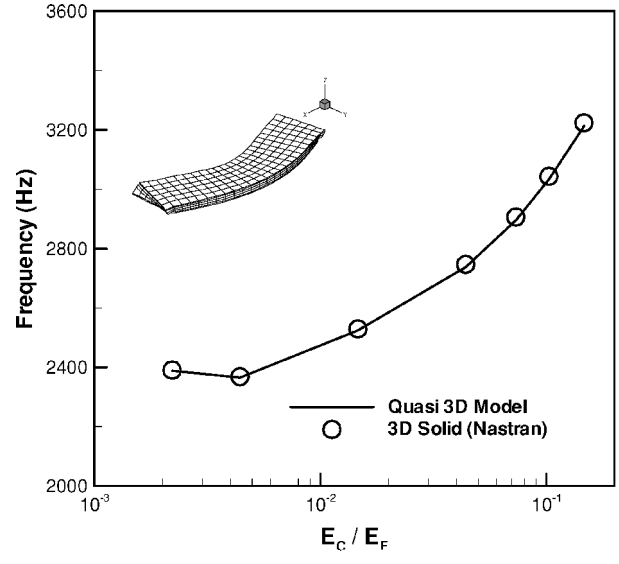

Fig. 12 First in-plane mode of bottom face sheet clamped for two opposite borders.

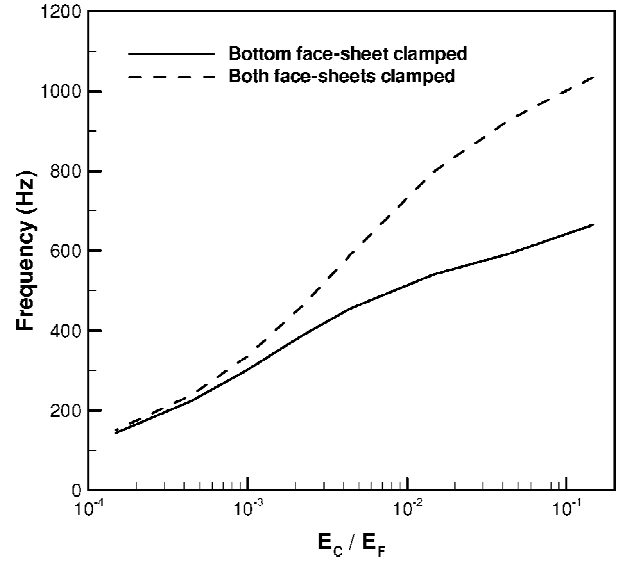

Fig. 13 Comparison for two different boundary conditions: first bending mode.

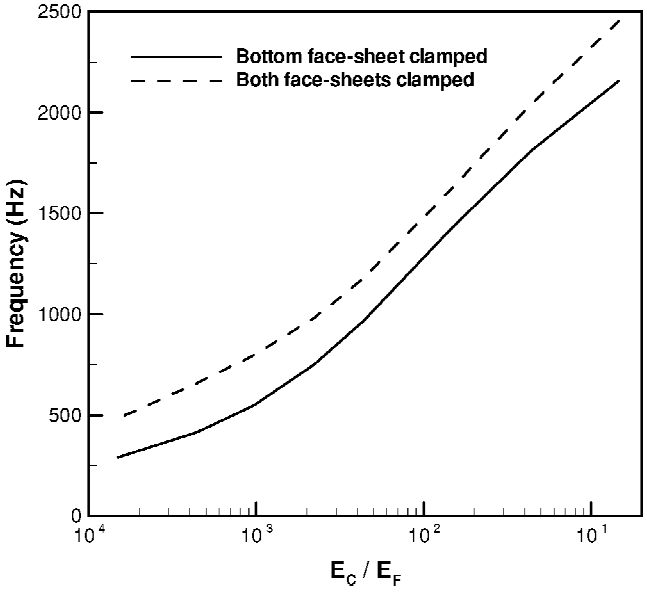

Fig. 14 Comparison for two different boundary conditions: first torsion mode.

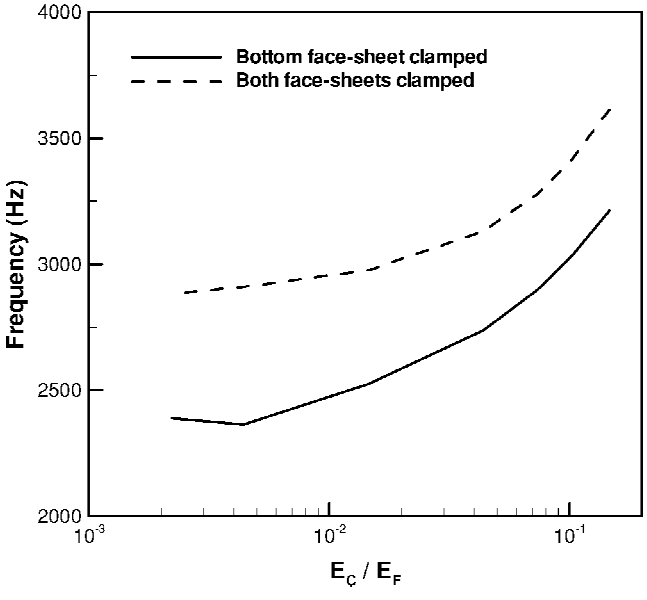

Fig. 15 Comparison for two different boundary conditions: first in-plane mode.

between the quasi-three-dimensional model and three-dimensional Nastran results.

The boundary condition study is continued in Figs. 13–15. A comparison for plates with two opposite edges clamped is made. In these results natural frequencies are obtained for the bottom face sheet clamped and for the both face sheets clamped. The first bending mode comparison shows the great changes resulting for different boundary conditions. The current quasi-three-dimensional formulation is again shown to yield accurate solutions compared to the full three-dimensional calculations.

Conclusions

Oskooei and Hansen[11] showed that the three-layer quasi-three-dimensional model provided an accurate and robust tool for the static analysis of the sandwich plates. In the current work excellent results are obtained for the natural frequencies and free-vibration modes compared to three-dimensional Nastran calculations. The current approach yields excellent results even for sandwich plates with large differences between the core and face-sheet transverse stiffness, and this accuracy is not influenced by the plate boundary conditions.

Finally, the through-thickness plate geometry does not affect the number of degrees of freedom of a quasi-three-dimensional model; however, if the face sheets are thin a three-dimensional solid model requires an excessive number of through-thickness elements to overcome numerical difficulties resulting from poor element aspect ratio. Therefore, when thin face sheets are modeled in a sandwich structure the current quasi-three-dimensional model can have some distinct computational advantages in comparison to a usual three-dimensional finite element model. The current calculations illustrate that the present model obtains accurate solutions even with a small number of elements.

Acknowledgments

The authors acknowledge the CNPq (Brazilian National Research Council) under Grant 300219/90-3 and the Fundação de Amparo à Pesquisa do Estado de São Paulo under Grant 1998/12608-1 for the financial support received for this work.

References

[1]Reissner, E., "Finite Deflection of Sandwich Plates," *Journal of Aerospace Science*, Vol. 15, No. 7, 1948, pp. 435–440.

[2]Allen, H. G., *Analysis and Design of Structural Sandwich Panels*, Pergamon, Oxford, 1969, Chap. 2.

[3]Plantema, F. J., *Sandwich Construction*, Wiley, New York, 1966.

[4]Ojalvo, I. V., "Departures from Classical Beam Theory in Laminated Sandwich and Short Beams," *AIAA Journal*, Vol. 15, No. 10, 1977, pp. 1518–1521.

[5]Holt, D. J., and Webber, J. P. H., "Exact Solution to Some Honeycomb Sandwich Beam, Plate and Shell Problems," *Journal of Strain Analysis*, Vol. 17, No. 1, 1982, pp. 1–8.

[6]Monforton, G. R., and Ibrahim, I. M., "Modified Stiffness Formulation of Unbalanced Anisotropic Sandwich Plates," *International Journal of Mechanical Science*, Vol. 19, 1977, pp. 335–343.

[7]Frostig, Y., Baruch, M., and Vilnay, O., "A High Order Theory for the Bending of Sandwich Beams with a Flexible Core," *Journal of Engineering Mechanics*, Vol. 118, No. 5, 1992, pp. 1026–1043.

[8]Frostig, Y., and Baruch, M., "Vibration of Sandwich Beams—A High Order Theory Approach," *Journal of Sound and Vibration*, Vol. 176, No. 2, 1994, pp. 195–208.

[9]Frostig, Y., and Baruch, M., "Localized Load Effects in High-Order Bending of Sandwich Plates with Flexible Core," *Journal of Engineering Mechanics*, Vol. 122, No. 11, 1996, pp. 1069–1076.

[10]Thomsen, O. T., "Analysis of Local Bending Effects in Sandwich Plates with Orthotropic Face Layers Subjected to Localized Loads," *Composite Structures*, Vol. 25, 1993, pp. 511–520.

[11]Oskooei, S., and Hansen, J. S., "Higher-Order Finite Element for Sandwich Plates," *AIAA Journal*, Vol. 38, No. 3, 2000, pp. 525–533.

[12]Jones, R. M., *Mechanics of Composite Materials*, Scripta, Washington, DC, 1975, Chap. 4.

[13]Heppler, G. R., and Hansen, J. S., "A Mindlin Element for Thick and Deep Shells," *Computational Methods in Applied Mechanical Engineering*, Vol. 54, No. 1, 1986, pp. 21–47.

[14]Nabarrete, A., "A Three Layer Quasi 3D Finite Element Model for Structural Analysis of Sandwich Plates," Ph.D. Dissertation, Dept. of Mechanical Engineering, Instituto Tecnológico da Aeronáutica, Saõ José dos Campos, Brazil, May 2002.

[15]Bathe, K.-J., *Finite Element Procedures*, Prentice–Hall, Upper Saddle River, NJ, 1996, Chap. 6.

[16]Hernandes, J. A., Almeida, S. F. M., and Nabarrete, A., "Stiffening Effects on the Free Vibration Behavior of Composite Plates with PZT Actuators," *Composite Structures*, Vol. 49, 2000, pp. 55–63.

A. Berman
Associate Editor